

## BASIC ANALYSES OF DOME FUJI DEEP ICE CORE PART 2: PHYSICAL PROPERTIES

Takeo HONDOH<sup>1</sup>, Hideki NARITA<sup>1</sup>, Akira HORI<sup>1</sup>, Michiko FUJII<sup>2</sup>,  
Hitoshi SHOJI<sup>3</sup>, Takao KAMEDA<sup>3</sup>, Shinji MAE<sup>4</sup>, Shuji FUJITA<sup>4</sup>,  
Tomoko IKEDA<sup>4</sup>, Hiroshi FUKAZAWA<sup>4</sup>, Taku FUKUMURA<sup>4</sup>,  
Nobuhiko AZUMA<sup>5</sup>, Y. WONG<sup>5</sup>, Kunio KAWADA<sup>6</sup>,  
Okitsugu WATANABE<sup>7</sup> and Hideaki MOTOYAMA<sup>7</sup>

<sup>1</sup> *Institute of Low Temperature Science, Hokkaido University, Kita-19, Nishi-8,  
Kita-ku, Sapporo 060-0819*

<sup>2</sup> *Graduate School of Environmental Earth Science, Hokkaido University,  
Kita-10, Nishi-5, Kita-ku, Sapporo 060-0810*

<sup>3</sup> *Kitami Institute of Technology, Koen-cho, Kitami 090-0015*

<sup>4</sup> *Department of Applied Physics, Hokkaido University, Kita-13, Nishi-8,  
Kita-ku, Sapporo 060-8628*

<sup>5</sup> *Nagaoka University of Technology, 1603-1 Kamitomioka-cho, Nagaoka 940-2137*

<sup>6</sup> *Department of Earth Science, Toyama University, 3190 Gofuku, Toyama 930-0887*

<sup>7</sup> *National Institute of Polar Research, Kaga 1-chome, Itabashi-ku, Tokyo 173-8515*

**Abstract:** Physical analyses of the Dome Fuji ice core have been carried out to reveal fundamental properties of the core: (1) Stratigraphy, (2) Bulk density by a volumetric method, (3) Bulk density by an x-ray transmission method, (4) Total gas content, (5) Permeability and bubble volume, (6) Distribution of air-bubbles, (7) Distribution of clathrate hydrates, (8) Raman spectral N<sub>2</sub>/O<sub>2</sub> ratios of air-bubbles and clathrate hydrates, (9) Ice fabrics, (10) Ice grain size, (11) Laser scattering tomography, (12) DC-ECM and AC-ECM, (13) Mechanical test, and (14) Crystalline structures of ice and clathrate hydrate. In the present paper the main results obtained so far are summarized.

### 1. Introduction

A continuous 2503 m long ice core was recovered at the summit of Dome Fuji Station, Antarctica, during the years 1993–1997 (DOME-F DEEP ICE CORING GROUP, 1998). This ice core is expected to provide paleoclimate and paleoenvironment records over 300000 years (DOME-F ICE CORE RESEARCH GROUP, 1998; WATANABE *et al.*, 1999). In order to obtain depth profiles of fundamental chemical and physical properties of the core, basic analyses have been carried out by the Dome-F Ice Core Research Group during the last two years. In the present paper entitled “Basic analyses of Dome Fuji deep ice core. Part 2: Physical properties”, we describe the results of the basic analysis program of Dome Fuji Ice Core Drilling Project obtained by December 1998. Details of the individual data sets and discussions on the data will be given in other papers to be prepared by the proper authors.

## 2. Sample Preparation

The ice cores were vertically slit at the Dome Fuji Station as shown in Fig. 1. Electrical conductivity measurements, DC- and AC-ECM, were carried out on a fresh surface of A-cores at the station (DOME-F DEEP ICE CORING GROUP, 1998). Both B- and C-cores were shipped to Japan, and are being kept in cold rooms of the Institute of Low Temperature Science (ILTS) and of the National Institute of Polar Research (NIPR), respectively. B-cores are mainly used for physical analyses, and are being kept at  $-50^{\circ}\text{C}$  to avoid dissociation of air-hydrate crystals. For measurements of ice fabrics and ice grain-size and other optical microscope observations, vertical thin sections of the ice cores have been prepared from the B-cores as shown in Fig. 1.

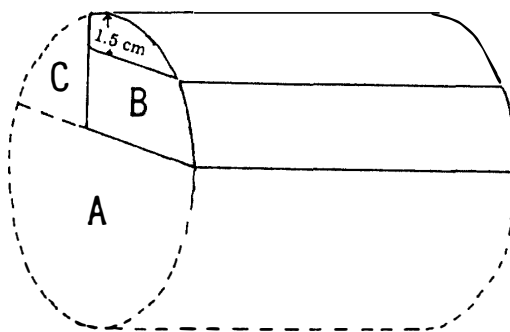


Fig. 1. A schematic illustration of ice core sampling. Physical analyses have been carried out using a sector B slit from a cylindrical core with a diameter of about 95 mm.

## 3. New Methods

We have introduced several new methods and techniques for Dome Fuji core analyses in order to obtain new information from the cores. We also aimed to clarify various microphysical processes that affect formation and modification of the ice-core records. The following methods have been introduced in the physical analyses: (1) AC-ECM for impurity distributions; (2) X-ray transmission method for bulk density; (3) Raman spectral method for local distribution of gaseous molecules; (4) Automatic fabric analyzer for rapid analyses; (5) Laser scattering tomography for distribution of inclusions; (6) Neutron scattering method and x-ray diffraction method for crystal structures. The details of the methods have been given in the separate papers, or will be given elsewhere.

## 4. Results of the Basic Analyses

### 4.1. Stratigraphy

Stratigraphical observations were carried out at both the Dome Fuji Station and the ILTS laboratory. At Dome Fuji Station, distributions of breaks, tephra layers and cloudy bands were recorded. By careful observations in the ILTS laboratory, a

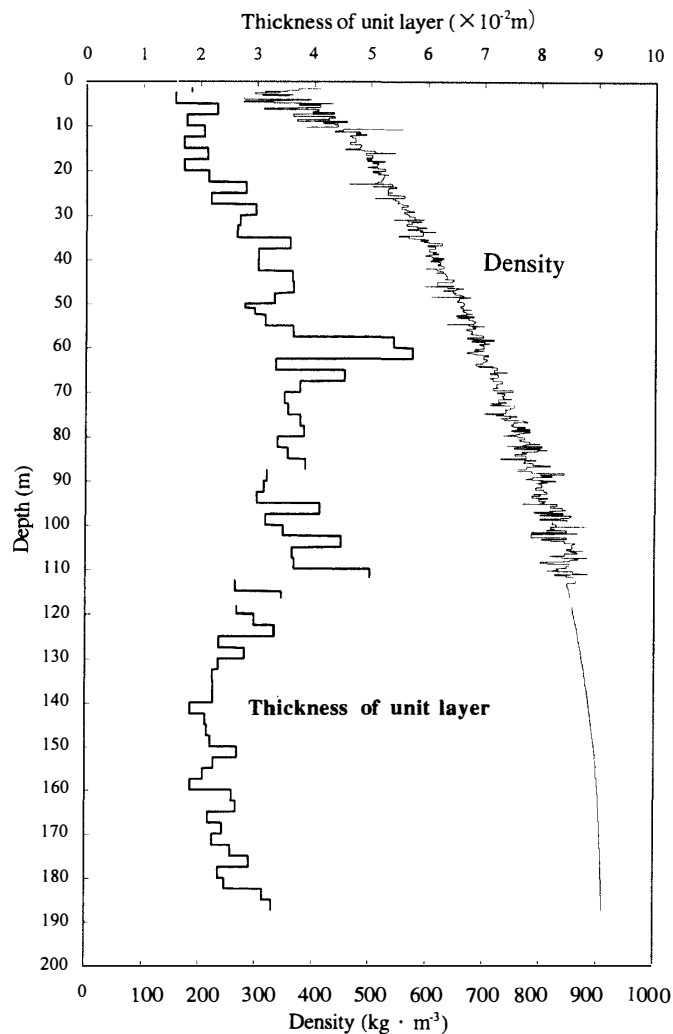


Fig. 2. Thickness of stratigraphical layers and bulk density profile.

characteristic layer structure was found in the shallow part of the cores, and the thickness or periodicity of the structure was measured. Figure 2 shows the water equivalent thickness of the layer as a function of depth down to 190 m (NARITA *et al.*, in preparation). The average layer thickness is 28 mm, which is close to the present accumulation rate. This variation of layer thickness probably suggests a change in accumulation rates in the last 5000 years.

#### 4.2. Density of cores

Bulk density was measured by a volumetric method (measuring weight and size of the cores) at Dome Fuji Station. The result is shown in Fig. 2. A close-off density of  $0.83 \text{ Mg} \cdot \text{m}^{-3}$  is reached at around 100 m depth. More precise measurement on the density was also carried out by the hydrostatic method using isooctane as the liquid bath. The obtained data are given in Table 1 and in Fig. 3. The large increase in density from 500 m to 1200 m is attributed to transformation from air bubbles to air hydrates (see Fig. 6).

Table 1. Precise bulk densities measured by the hydrostatic method at the drilling site in January 1997.

Depth (m)		Density ( $\pm 0.3 \text{ kg} \cdot \text{m}^{-3}$ )	Time after the drilling (months)
from	to		
500.81	500.85	917.9	12
850.02	850.06	919.1	8
1200.46	1200.50	920.1	6
1550.46	1550.50	920.2	5
1900.46	1900.50	920.3	4
2250.00	2250.04	920.3	1

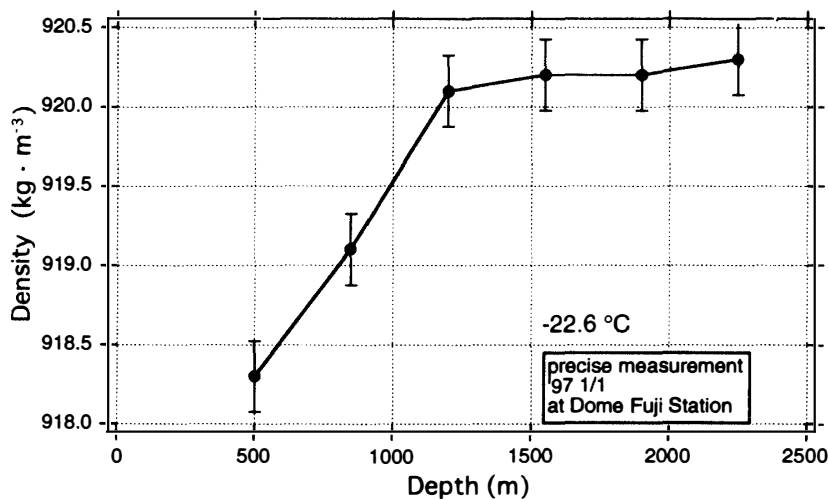


Fig. 3. Precise bulk densities of deep ice cores measured by the hydrostatic method.

Bulk density was also measured by an X-ray transmission method in the ILTS laboratory. In this method, intensities of X-rays transmitted through a thick ice-core sample were continuously measured to obtain a detailed density profile with a spatial resolution down to 1 mm. An advantage of this method is that periodic fluctuation in density as well as core layer structure was found (for details, see HORI *et al.*, 1999).

#### 4.3. Total air content and bubble volume

Bubble volumes were measured by a classical method based on the Boyle-Mariottes law for an ideal gas (KAMEDA and NARUSE, 1994); and the results are shown in Fig. 4. Air bubbles isolated from air channels are formed in the depth range from 90 m to 110 m as shown in the figure.

Figure 5 shows total air content of ice measured by a melting method (LANGWAY, 1958). The air contents in Holocene ice are smaller by 14% than those of ice at the last glacial maximum (LGM). If we assume that the air content depends on either close-off elevation or porosity of ice at pore close-off depth, this result suggests either thickening of the ice sheet or increase of the porosity during the transition from the LGM to the Holocene (KAMEDA *et al.*, in preparation).

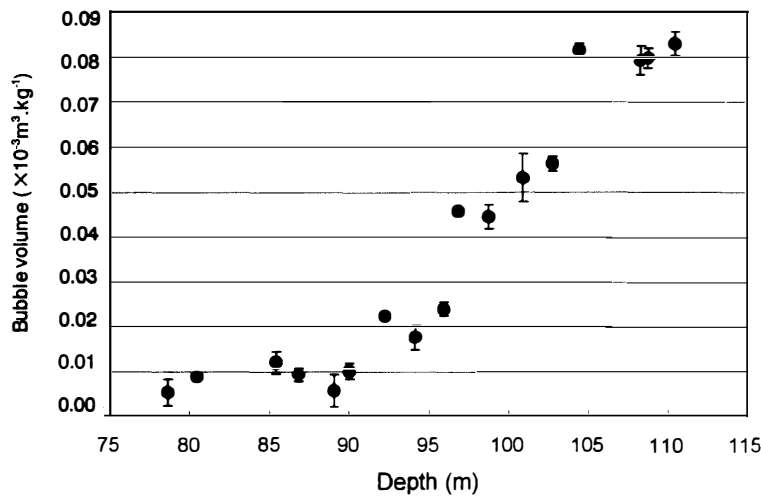


Fig. 4. Bubble volume of firm ice.

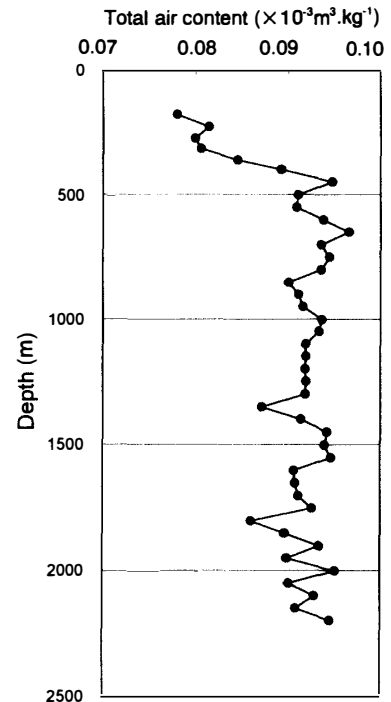


Fig. 5. Total air content profile.

#### 4.4. Distribution of air-bubbles and clathrate hydrates

Figure 6 shows the number and size of air-bubbles and clathrate hydrates measured by optical microscope observations and laser scattering tomography (NARITA *et al.*, 1999). As transition from bubbles to hydrates, the number concentration of air-bubbles gradually decreased and finally disappeared at 1100m. The first hydrate

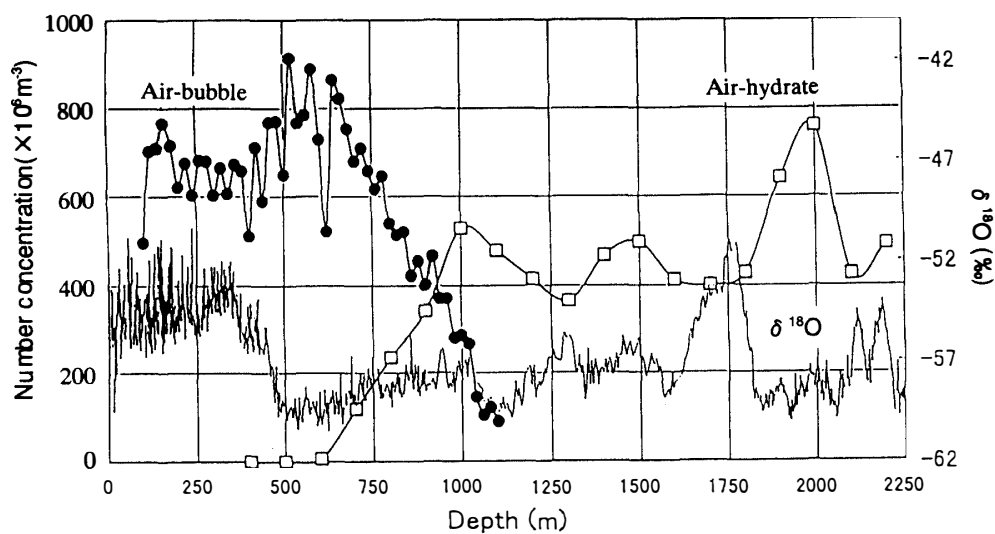


Fig. 6. Number concentrations of air-bubbles and air-hydrates. The  $\delta^{18}\text{O}$  profile (bottom curve) is also shown for reference.

crystal was found at 550 m, and the number concentrations of the hydrates increased with depth. The transition zone at Dome Fuji Station is therefore from 550 m to 1100 m. Above and below the transition zone, the fluctuation of the number concentrations seems to correlate with  $\delta^{18}\text{O}$  although more data at shorter intervals are required for further discussion of the phenomenon (for details, see NARITA *et al.*, 1999).

To observe distribution of inclusions such as air-bubbles, air-hydrates and other particles, laser scattering tomography was used. Layer structure was found in the distribution of air-bubbles and air-hydrates. From the detailed profile of the number densities of air-hydrates, we found a periodic fluctuation in the number densities of which periodicity decreases with depth. Since such a non-uniform distribution of air-hydrates is attributed to non-uniform distribution of air-bubbles, the periodicity probably corresponds to stratigraphical periodicity found in the shallow part. This fact offers us a new method to deduce accumulation rates along the whole length of the Dome Fuji core (NARITA *et al.*, in preparation).

#### 4.5. Raman spectral $\text{N}_2/\text{O}_2$ ratios of air-bubbles and clathrate hydrates

Raman spectral method was first applied to Vostok ice cores, and systematic changes in  $\text{N}_2/\text{O}_2$  ratios of air-bubbles and clathrate hydrates were found (IKEDA *et al.*, 1999). Similar fractionation was also confirmed in Dome Fuji ice cores (FUKUMURA *et al.*, in preparation). This phenomenon was well explained in terms of diffusive flow of  $\text{N}_2$  and  $\text{O}_2$  molecules through ice (IKEDA *et al.*, 1999). We have to take this fractionation effect into consideration in paleoatmospheric reconstruction from gas analyses data.

#### 4.6. Textures and fabrics

Crystal *c*-axis orientations, and sizes and aspect ratios of crystal grains, were

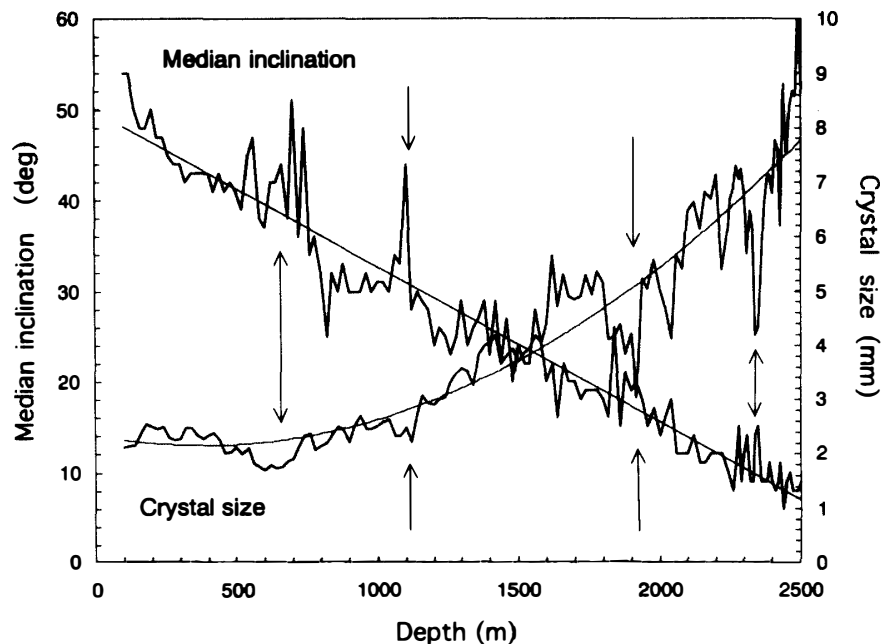


Fig. 7. Depth profiles of crystal sizes and crystal orientations (median inclinations).

measured by the use of an automatic fabric analyzer developed by AZUMA *et al.* (1999) and WANG and AZUMA (1999). Using this new powerful tool, a large number of samples have been analyzed in a rather short period without laborious work in a cold room. As depth increases, mean crystal size increases and median inclination decreases as shown in Fig. 7. This change in orientation distribution of *c*-axes means that crystals rotate toward vertical orientation by vertical compressive stresses to form typical single-maximum fabrics. Differences from the average in both crystal size and median inclination correlate well with the  $\delta^{18}\text{O}$  profile (for details, see AZUMA *et al.*, 1999).

#### 4.7. DC-ECM and AC-ECM

The ECM technique (DC-ECM) developed by HAMMER (1983) is one of the

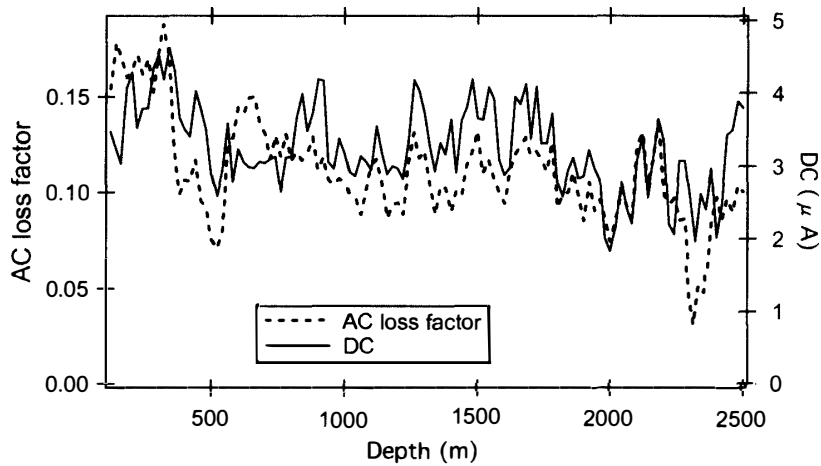


Fig. 8. DC-ECM profile (right axis) and AC-ECM loss factor profile (left axis). The plotted data were averaged over the 20 m length of the cores using the original data digitized at every 2 mm. Data measured at different temperatures were converted to those at  $-25^{\circ}\text{C}$  using an activation energy of 0.248 eV.

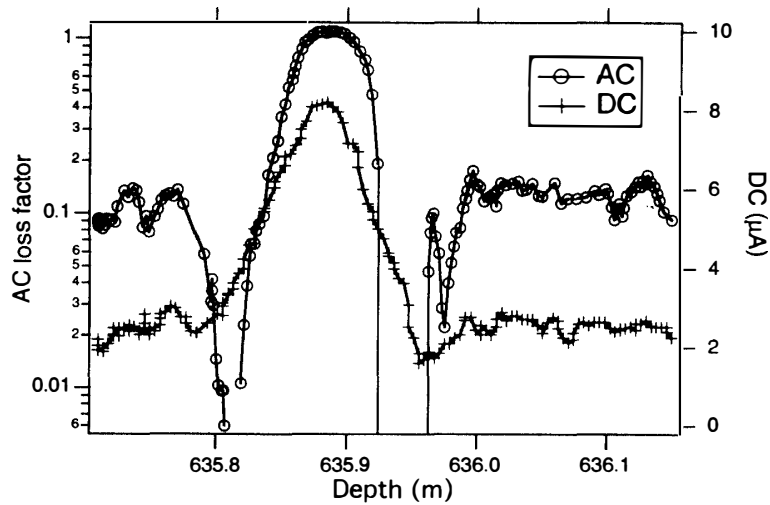


Fig. 9. Comparison of AC-ECM and DC-ECM signals around a volcanic peak event.

standard methods for ice core analyses to observe distribution of acidity along the whole length of ice cores. In this method, a continuous profile of DC currents is recorded by scanning two electrodes on the ice surface. In contrast, an AC current profile is recorded by a new AC-ECM technique. This new method permits us to observe the distributions of both basic and acid impurities (SUGIYAMA *et al.*, 1995).

Figure 8 shows both DC- and AC-ECM profiles along the whole length of the Dome Fuji core. For DC-ECM measurements, high voltage of 1250 V was applied on the ice surface through two electrodes separated by 15 mm. In contrast, AC electrical field of 1 V at 1 MHz was applied in case of AC-ECM measurements. Although similar changes can be seen in the two profiles below 800 m depth, significant difference was also found. For a typical example, Fig. 9 shows a comparison of these two profiles around a volcanic peak. The AC loss factors have two sharp negative peaks at both sides of the positive peak. Although careful investigations are needed to reveal the origin of the differences, these comparisons offer a new tool to find unknown paleoenvironmental events.

#### 4.8. Mechanical test

Mechanical tests are being carried out to clarify the deformation (plasticity) parameter *B* as a function of depth. Since single maximum fabrics are well developed in the deeper part of the cores, strong anisotropy of plasticity is expected.

#### 4.9. Crystalline structures of ice and clathrate hydrate

Neutron scattering data on Dome Fuji ice (FUKAZAWA *et al.*, 1998, 1999b) and Vostok ice (FUKAZAWA *et al.*, 1999a) strongly suggest a new phase of ice. This finding implies a very slow phase transition of ice that cannot be observed in the laboratory. X-ray diffraction experiments as well as Raman scattering and neutron diffraction experiments are being carried out to reveal the structure of the new phase.

### 5. Concluding remarks

Depth profiles of physical properties of the Dome Fuji core are presented. For further development of ice core research, the following points should be emphasized.

- (1) Fabric development in the summit core was well established.
- (2) Correlation between ice grain-size and  $\delta^{18}\text{O}$  was found.
- (3) Density fluctuations were found in firn ice by the x-ray transmission method.
- (4) Variation in thickness of stratigraphical layers was found in the shallow part.
- (5) Layer structures in the deeper part were also found to appear as periodic fluctuations in number densities of air-bubbles and air-hydrates.
- (6) All of the periodicities found in (3) to (5) are close to the annual layer thicknesses estimated; therefore, this fact offers a new method to obtain annual accumulation rates over a whole core length.
- (7) A very large fractionation of gaseous molecules caused by transition from air-bubbles to air-hydrates was confirmed.
- (8) AC-ECM was proved to detect distribution of chemicals other than acidity.

## References

- AZUMA, N., WANG, Y., MORI, K., NARITA, H., HONDOH, T., SHOJI, H. and WATANABE, O. (1999): Textures and fabrics in the Dome F ice core. *Ann. Glaciol.*, **29** (in press).
- DOME-F DEEP ICE CORING GROUP (1998): Deep ice-core drilling at Dome Fuji and glaciological studies in east Dronning Maud Land, Antarctica. *Ann. Glaciol.*, **27**, 333–337.
- DOME-F ICE CORE RESEARCH GROUP (1998): Preliminary investigation of paleoclimate signals recorded in the ice core from Dome Fuji Station, east Dronning Maud Land, Antarctica. *Ann. Glaciol.*, **27**, 338–342.
- FUKAZAWA, H., MAE, S., IKEDA, S. and WATANABE, O. (1998): Proton ordering in Antarctic ice observed by Raman and Neutron scattering. *Chem. Phys. Lett.*, **294**, 554–558.
- FUKAZAWA, H., MAE, S., IKEDA, S. and LIPENKOV, V., Ya. (1999a): Neutron scattering measurements on Vostok Antarctic ice. *Polar Meteorol. Glaciol.*, **13**, 75–82.
- FUKAZAWA, H., MAE, S., IKEDA, S. and WATANABE, O. (1999b): Incoherent inelastic neutron scattering measurements on Dome Fuji Antarctic ice. *Earth Planet. Sci. Lett.* (in press).
- HAMMER, C.U. (1983): Initial direct current in the buildup of space charges and acidity of the cores. *J. Phys. Chem.*, **87**, 4099–4103.
- HORI, A., TAYUKI, K., NARITA, H., HONDOH, T., FUJITA, S., KAMEDA, T., SHOJI, H., AZUMA, N., KAMIYAMA, K., FUJII, Y., MOTOYAMA, H., and WATANABE, O. (1999): A detailed density profile of the Dome Fuji shallow ice core by X-ray transmission method. *Ann. Glaciol.*, **29** (in press).
- IKEDA, T., FUKAZAWA, H., MAE, S., PEPIN, L., DUVAL, P., CHAMPAGNON, B., LIPENKOV, V. Ya. and HONDOH, T. (1999): Extreme fractionation of gases caused by formation of clathrate hydrates in Vostok Antarctic ice. *Geophys. Res. Lett.*, **26**, 91–94.
- KAMEDA, T. and NARUSE, R. (1994): Characteristics of bubble volumes in firn-ice transition layers of ice cores from polar ice sheets. *Ann. Glaciol.*, **20**, 95–100.
- LANGWAY, C.C., Jr. (1958): Bubble pressure in Greenland glacier ice. *International Association of Scientific Hydrology, Publication No. 47*, 336–349.
- NARITA, H., AZUMA, N., HONDOH, T., FUJII, M., KAWAGUCHI, M., MAE, S., SHOJI, H., KAMEDA, T. and WATANABE, O. (1999): Characteristics of air bubbles and hydrates in the Dome F ice core, Antarctica. *Ann. Glaciol.*, **29** (in press).
- SUGIYAMA, K., FUJITA, S., SUEOKA, S., MAE, S. and HONDOH, T. (1995): Preliminary measurement of high-frequency electrical conductivity of Antarctic ice with AC-ECM technique. *Proc. NIPR Symp. Polar Meteorol. Glaciol.*, **9**, 12–22.
- WANG, Y. and AZUMA, N. (1999): The development of an automatic fabric analyzer by image-analysis techniques. *Ann. Glaciol.*, **29** (in press).
- WATANABE, O., FUJII, Y., KAMIYAMA, K., MOTOYAMA, H., FURUKAWA, T., IGARASHI, M., KOHNO, M., KANAMORI, S., KANAMORI, N., AGETA, Y., NAKAWO, M., TANAKA, H., SATOW, K., SHOJI, H., KAWAMURA, K., MATOBA, S. and SHIMADA, W. (1999): Basic analyses of Dome Fuji deep ice core. Part 1: Stable oxygen and hydrogen isotope ratios, major chemical compositions and dust concentration. *Polar Meteorol. Glaciol.*, **13**, 83–89.

*(Received May 1, 1999; Revised manuscript accepted September 22, 1999)*